Taylor & Francis
Taylor & Francis Group

Computer Methods in Biomechanics and Biomedical Engineering

ISSN: (Print) (Online) Journal homepage: https://www.tandfonline.com/loi/gcmb20

Artificial Intelligence-Assisted motion capture for medical applications: a comparative study between markerless and passive marker motion capture

Iwori Takeda , Atsushi Yamada & Hiroshi Onodera

To cite this article: Iwori Takeda , Atsushi Yamada & Hiroshi Onodera (2020): Artificial Intelligence-Assisted motion capture for medical applications: a comparative study between markerless and passive marker motion capture, Computer Methods in Biomechanics and Biomedical Engineering, DOI: 10.1080/10255842.2020.1856372

To link to this article: https://doi.org/10.1080/10255842.2020.1856372

Published online: 08 Dec 2020.

COMPUTER METHODS IN BIOMECHANICS AND BIOMEDICAL ENGINEERING
https://doi.org/10.1080/10255842.2020.1856372

Artificial Intelligence-Assisted motion capture for medical applications: a comparative study between markerless and passive marker motion capture

Iwori Takeda, Atsushi Yamada and Hiroshi Onodera

Department of Mechanical Systems Engineering, School of Engineering, The University of Tokyo, Tokyo, Japan

ABSTRACT

We aimed to determine whether artificial intelligence (AI)-assisted markerless motion capture software is useful in the clinical medicine and rehabilitation fields. Currently, it is unclear whether the AI-assisted markerless method can be applied to individuals with lower limb dysfunction, such as those using an ankle foot orthosis or a crutch. However, as many patients with lower limb paralysis and foot orthosis users lose metatarsophalangeal (MP) joint flexion during the stance phase, it is necessary to estimate the accuracy of foot recognition under fixed MP joint motion. The hip, knee, and ankle joint angles during treadmill walking were determined using OpenPose (a markerless method) and the conventional passive marker motion capture method; the results from both methods were compared. We also examined whether an ankle foot orthosis and a crutch could influence the recognition ability of OpenPose. The hip and knee joint data obtained by the passive marker method (MAC3D), OpenPose, and manual video analysis using Kinovea software showed significant correlation. Compared with the ankle joint data obtained by OpenPose and Kinovea, which were strongly correlated, those obtained by MAC3D presented a weaker correlation. OpenPose can be an adequate substitute for conventional passive marker motion capture for both normal gait and abnormal gait with an orthosis or a crutch. Furthermore, OpenPose is applicable to patients with impaired MP joint motion. The use of OpenPose can reduce the complexity and cost associated with conventional passive marker motion capture without compromising recognition accuracy.

ARTICLE HISTORY
Received 7 July 2020
Accepted 23 November 2020

KEYWORDS
Artificial intelligence; gait analysis; markerless motion capture; metatarsophalangeal joint; OpenPose

1. Introduction

Motion capture systems are commonly used in the medical science and rehabilitation fields to evaluate human motor function (Matić et al. 2016; Lee et al. 2017; McMulkin et al. 2019). The mainstream of motion capture is the passive optical method, in which the markers attached to the subject's body surface are tracked and the position of each part of the subject's body can be estimated from the three-dimensional coordinates of such markers. However, motion analysis using the passive marker motion capture (PMMC) system is laborious, as it involves complicated body marking, the adjustment of many cameras, and post processing. Most importantly, the conventional PMMC system cannot analyze the natural motion of patients in rehabilitation rooms or at home (Patterson et al. 2014; Saini et al. 2020).

Recently, artificial intelligence (AI)-assisted markerless motion capture software has been developed such as OpenPose, PoseNet, and AlphaPose (Kendall et al. 2015; Fang et al. 2017). The latest version of OpenPose can recognize the heel and toe positions, which are of value to analyze the abnormal gait of patients suffering from hemiparesis and neuropathy, because they show impaired motion in the ankle and metatarsophalangeal (MP) joints (Cao et al. 2017; Qiao et al. 2017). Thus, OpenPose can be a substitute for the conventional PMMC method (Mehrizi et al. 2019; Nakano et al. 2019; Slembrouck et al. 2020). However, few studies have compared conventional PMMC with AI-assisted markerless motion capture. Furthermore, it is not clear whether the AI-assisted markerless method can be applied to individuals with lower limb movement disorders, such as those using an ankle foot orthosis or a crutch. In this study, we compared the performance of conventional PMMC with that of OpenPose during treadmill walking. The walking direction on the treadmill was restricted to a two-dimensional plane in order to compare the joint angle data by OpenPose with those by the three-

CONTACT Iwori Takeda i_takeda@psc.t.u-tokyo.ac.jp

dimensional PMMC system. In addition, we examined the effect of an ankle foot orthosis and a crutch on the recognition ability of OpenPose. A common error that appears in OpenPose's analysis is also discussed.

2. Methods

We performed three walking tests: a normal test, a fixed MP joint test, and a simulated lower limb dysfunction test. Metal insoles were used to fix the foot MP joint. Figure 1(a) shows a schematic including the motion capture system, treadmill, and video camera. A healthy male subject (height: 1.75 m, weight: 55 kg) walked on the treadmill in the motion capture measurement room. We used MAC3D (Motion analysis Corp., Santa Rosa, CA, USA) as the PMMC system. Fourteen reflective markers were attached to the subject's body at the positions shown in Figure 1(b), and their three-dimensional coordinates were obtained at 60 Hz. We used Visual3D (C-Motion, Inc.; Germantown, MD, USA) for the three-dimensional motion analysis, and measured the joint angles of the lower limbs. The normal gait walking speed was set at 4.5 km/h (Alkjaer et al. 2001; Lichtwark et al. 2007; Dahlgren et al. 2010). In order to restrict the motion range of the MP joint, metal insoles were placed inside the shoes worn by the subject and the walking speed was set at 1.8 km/h. The subject wore an ankle foot orthosis (ToeOFF Short, Allard USA Inc., Rockaway, NJ, USA) on his left leg and held a Lofstrand crutch (black color or silver color) with his right hand (Figure 1(c) and (d)).

Treadmill walking was recorded simultaneously using the motion capture system and a video camera (EX-F1, CASIO Computer Co. Ltd., Tokyo, Japan). The video data were analyzed with OpenPose (ver. 1.5.0). OpenPose can detect a person from the input images and videos unlike the conventional PMMC method, which obtains the three-dimensional coordinates of markers attached to the subject's body surface. The coordinates of the parts called key points, such as the nose and hip joint, can be output. Based on these coordinate data, the motion data such as joint angles can be obtained. The direction of the treadmill was restricted to a two-dimensional plane on which the camera was focused, in order to compare the joint angle data obtained by OpenPose with those obtained by the three-dimensional PMMC system. The distance between the subject's body centerline and the video camera was 6750 mm, and the focal length of the camera was 80 mm (equivalent focal length: 35 mm). The distortion caused by the video camera lens can affect the accuracy of OpenPose's data. As shown in Figure 1(e), the grid pattern projected by the projector was recorded with the video camera from a distance of 6750 mm. The length of one grid unit was measured at the center region and peripheral region of the video camera image. At the edge region, the length of the grid unit increased by 1.9% vertically and 1% horizontally, compared with the center region. Therefore, barrel and pincushion distortions in the video camera used were negligible.

To assess the recognition accuracy of OpenPose, we used Kinovea software (version 0.8.27, Kinovea Open Source Project, www.kinovea.org) to measure manually the position of the subject's body parts by analyzing the same video data used by OpenPose; Kinovea is a motion analysis software used in fields such as sports and medical science (Post et al. 2018; Namba et al. 2020). In the measurement using Kinovea, the average value of three measurements was used.

OpenPose shows the coordinates of the human hip joint, knee joint, ankle joint, big toe, small toe, and heel. First, these body parts and their coordinates in the n-th video frame were defined as Hip (h_{xn}, h_{yn}), Knee (k_{xn}, k_{yn}), Ankle (a_{xn}, a_{yn}), Big Toe (b_{xn}, b_{yn}), Small Toe (s_{xn}, s_{yn}), and Heel (he_{xn}, he_{yn}), respectively. Then, a point called Lumbar (h_{xn}, 0)—located immediately above the hip joint—and an intermediate point called Toe (($b_{xn}+s_{xn}$)/2, ($b_{yn}+s_{yn}$)/2)—located between the big and small toes—were defined. As shown in Figure 2, the hip joint angles during extension and flexion were defined as

$$\text{Hip joint angle (extension)} = \text{Lumbar–Hip–Knee angle} - 180^\circ, \tag{1}$$

$$\text{Hip joint angle (flexion)} = 180^\circ - \text{Lumbar–Hip–Knee angle}, \tag{2}$$

respectively; the knee joint angle was defined as

$$\text{Knee joint angle} = 180^\circ - \text{Hip–Knee–Ankle angle}; \tag{3}$$

and the ankle joint angle was defined as

$$\text{Ankle joint angle} = 90^\circ - (\text{Knee–Ankle–Toe angle} - \text{Ankle–Toe–Heel angle}). \tag{4}$$

The intraclass correlation coefficient ICC (2,1) was used to verify the degree of agreement between the analysis results of the PMMC system (MAC3D), OpenPose, and Kinovea. To this end, the ICCs were judged by their values as 'poor' (<0.4), 'fair' (0.4–0.6),

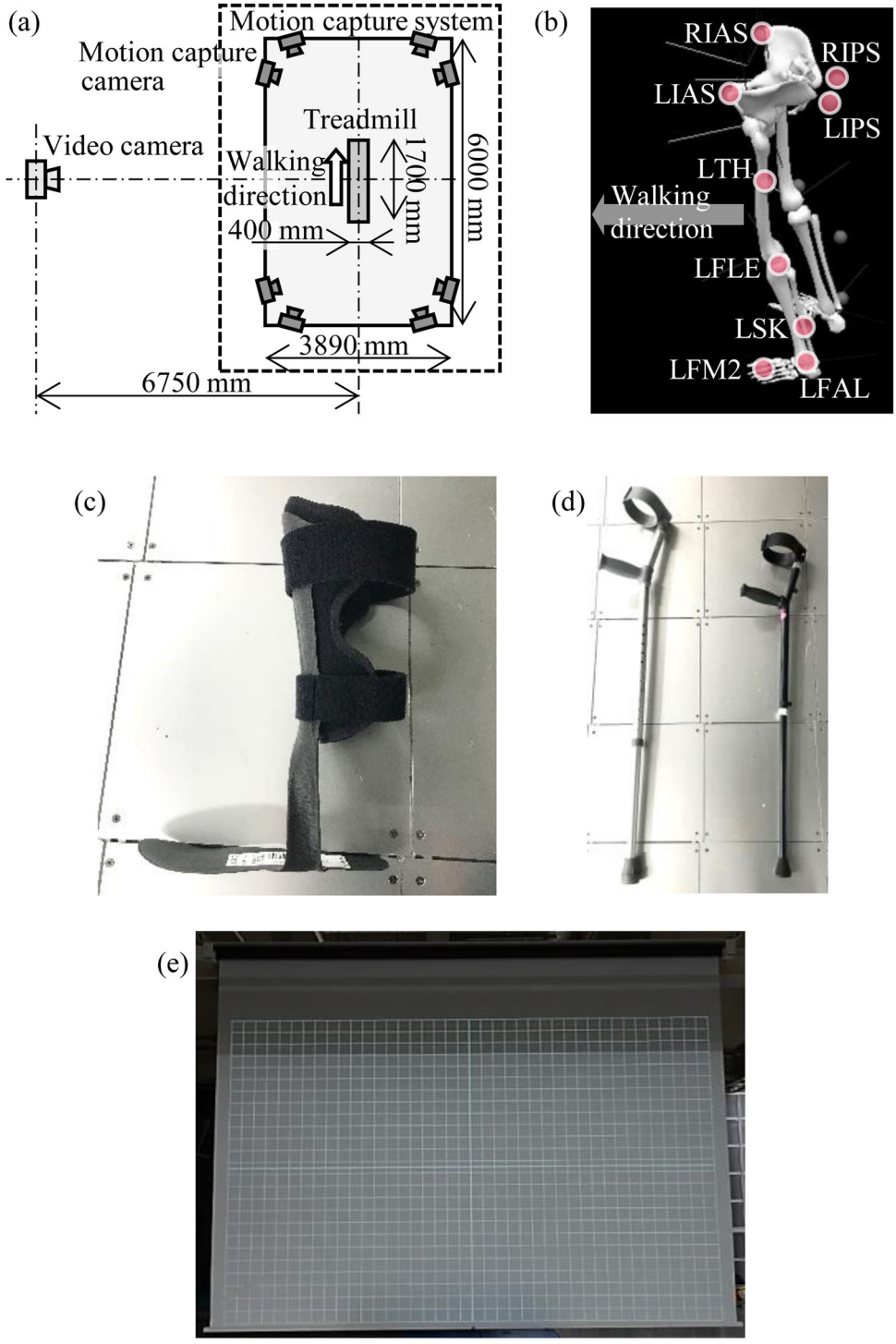

Figure 1. Experimental setup. (a) Overview of the motion capture system. (b) Marker placement for the motion capture experiments. Marker name and description of marker position are as follows: RIAS is right anterior superior iliac spine; LIAS is left anterior iliac spine; RIPS is right posterior superior iliac spine; LIPS is left posterior superior iliac spine; LTH is left thigh; LFLE is left femur lateral epicondyle; LSK is left shank; LFAL is left fibula apex of lateral malleolus; LFM2 is head of second metatarsus of left foot. (c) Ankle foot orthosis used on the subject's left leg and (d) black and silver Lofstrand crutches used on the subject's right upper limb to simulate gait disturbance owing to left lower limb dysfunction. (e) Grid pattern projected by the projector.

'good' (0.6–0.75), and 'excellent' (≥0.75) (Cicchetti 1994; Eltoukhy et al. 2017). All numerical analyses were performed using R version 2.8.1 (The R Development Core Team). The coordinate values of each joint obtained by OpenPose were smoothed using a five-point moving average filter. The joint angle data obtained from ten trials were analyzed and compared.

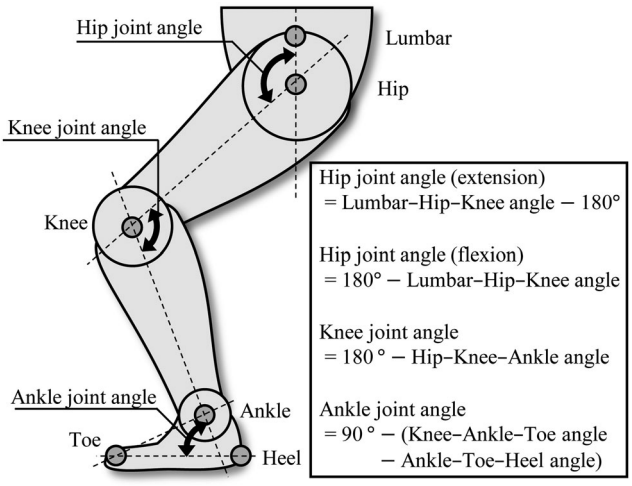

Figure 2. Definition of the hip, knee, and ankle joint angles (arrows) and calculation method. The joint angles in an upright standing position were defined as 0°.

3. Results

3.1. Normal gait

Figure 3 shows the left hip joint angles determined by the passive marker method, AI-assisted markerless method, and manual joint angle measurement using Kinovea. Figure 3(a) and (b) are ten superimposed gait cycles obtained by MAC3D and OpenPose, respectively. The changes in the hip joint angle during the gait cycle calculated from OpenPose's joint data were highly similar to those obtained by MAC3D and Kinovea. Figure 3(c) compares the typical gait cycles obtained by MAC3D, OpenPose, and Kinovea. The ICC (2,1) values of OpenPose and MAC3D for gait cycle intervals of 20% are shown in the graph; the ICC (2,1) values of the hip joint angle were high in all intervals. As shown in Table 1, the ICC (2,1) values in the entire gait cycle were 0.97, 0.96, and 0.98 for MAC3D and OpenPose, MAC3D and Kinovea, OpenPose and Kinovea, respectively. Figure 3(d) shows the leg positions during one gait cycle.

Figure 4 shows the left knee joint angles determined by MAC3D, OpenPose, and Kinovea. Figure 4(a) and (b) are ten superimposed gait cycles obtained by MAC3D and OpenPose, respectively. The changes in the knee joint angle during the gait cycle calculated from OpenPose's joint data were similar to those obtained by MAC3D and Kinovea. However, note that the small peak at 20% of the gait cycle seen in MAC3D was not seen in OpenPose. As shown in Figure 4(c), MAC3D, OpenPose, and Kinovea showed significantly similar knee joint angles in a typical gait cycle. The ICC (2,1) values of OpenPose and MAC3D for gait cycle intervals of 20% are shown in the graph;

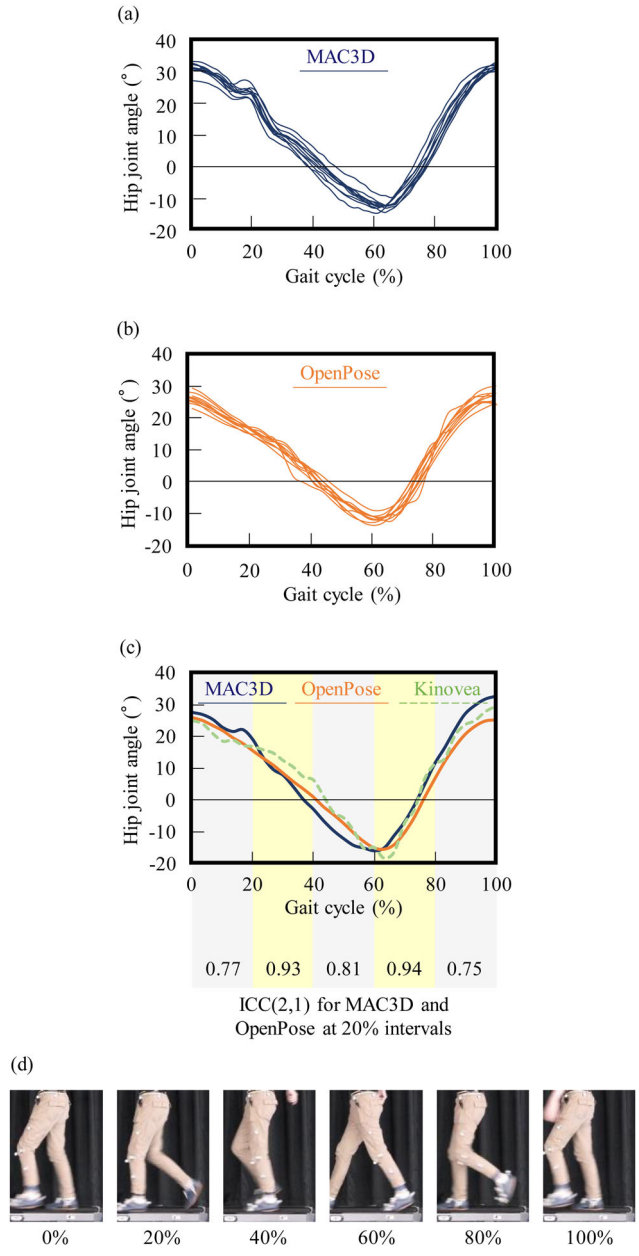

Figure 3. Left hip joint angle results. (a), (b) Ten superimposed gait cycles produced by MAC3D and OpenPose, respectively. (c) Superimposed left hip joint angles of a typical gait obtained by MAC3D, OpenPose, and Kinovea. (d) Photographs of a gait cycle.

the correlation was weak in the 0–60% region and strong in the 60–100% region. As shown in Table 1, the ICC (2,1) values in the entire gait cycle were 0.92, 0.90, and 0.98 for MAC3D and OpenPose, MAC3D and Kinovea, and OpenPose and Kinovea, respectively. The analysis results of the knee joint angle showed a strong correlation throughout the gait cycle.

Figure 5 shows the left ankle joint angles determined by MAC3D, OpenPose, and Kinovea. Figure 5(a) and (b) are ten superimposed gait cycles obtained by MAC3D and OpenPose, respectively. Figure 5(c)

Table 1. Intraclass correlation coefficients ICC(2,1) between the analysis results of MAC3D, OpenPose, and Kinovea.

	Hip joint		Knee joint		Ankle joint	
	OpenPose	Kinovea	OpenPose	Kinovea	OpenPose	Kinovea
MAC3D	0.97	0.96	0.92	0.90	0.51	0.57
OpenPose	–	0.98	–	0.98	–	0.87

shows a comparison between the typical gait cycles obtained by MAC3D, OpenPose, and Kinovea. In contrast to the results of the hip and knee joint angle changes, the ICC (2,1) values of the ankle joint angle for MAC3D and OpenPose were low in all gait phases. The ICC (2,1) values in the entire gait cycle were 0.51, 0.57, and 0.87 for MAC3D and OpenPose, MAC3D and Kinovea, and OpenPose and Kinovea, respectively, as shown in Table 1. Compared with the data obtained by OpenPose and Kinovea, which showed a strong correlation, the data obtained by MAC3D showed a poor correlation.

3.2. Simulated lower limb dysfunction

The gait in people with lower limb dysfunction differs from that of healthy people in several ways. For example, in the case of hemiparetic gait owing to stroke sequelae, the ankle joint dorsiflexion is insufficient on the affected side, resulting in a foot drop; therefore, many patients wear ankle foot orthoses to improve gait. However, the ankle foot orthosis limits the range of motion of the ankle and MP joints. The MP joint flexes greatly during the terminal stance phase (approximately 40–60% of the gait cycle) of normal gait (Figure 6(a)). Therefore, we investigated whether the restriction of the MP joint movement affects the recognition accuracy of OpenPose. The subject wore shoes with metal insoles to fix the MP joint during walking, as shown in Figure 6(b). In the case of Figure 6(a), the definition of ankle joint angle shown in Figure 2 cannot be applied, and the calculated ankle joint angle deviates from the actual value (Figure 6 (c)). Therefore, for the fixed MP joint condition, we expected the correlation between the analysis results of OpenPose and MAC3D for the terminal stance phase to be better than that shown in Figure 5(c). The walking speed was set to 1.8 km/h for safety; a gait at the natural walking speed (4.5 km/h) was practically impossible. The Ankle–Toe–Heel angle remains constant under the condition of fixed MP joint (Figure 2). Therefore, we determined the ankle joint angle with the Ankle–Toe–Heel angle adopting a constant value of 17° (Figure 6(d)); this value was selected as specific to this subject based on the measurement data obtained using Kinovea. Figure 6(e) shows the left ankle joint angles of a typical gait cycle determined by MAC3D and OpenPose under the fixed MP joint condition. MAC3D and OpenPose showed similar ankle joint angle change profiles; the ICC (2,1) values were 0.75 in the entire gait cycle and 0.29 in the 40–60% gait cycle region, which were higher than the results obtained without MP joint restriction (Figure 5(c)).

Patients with gait dysfunction often use a cane or a crutch together with an ankle foot orthosis. Figure 7 shows OpenPose's body part recognition results when the subject walked using a silver or black Lofstrand crutch on his right upper limb and wearing an ankle foot orthosis on his left leg (Figure 7 (a)). OpenPose correctly recognized the hip, knee, and ankle joint positions, and false crutch or orthosis recognition was not observed. The color of the crutch (silver or black) did not influence the recognition of each joint.

It is worth mentioning that an OpenPose recognition error was identified. As shown in Figure 8, the right and left feet were sometimes recognized reversely. Wearing tight pants can sometimes help to reduce the occurrence of this error, making leg recognition easier for OpenPose. In this study, we adopted this approach. There were also errors of key points not being detected. The output coordinates were zero in such cases, which made it easy to eliminate them. Because the analysis results of Kinovea and OpenPose were similar, it is believed that the Kinovea's data will be useful for identifying the errors of OpenPose. However, Kinovea's error correction is a manual process, which is very complicated and time consuming.

4. Discussion

Human motion analysis provides important information for the evaluation of rehabilitation progress and occupational safety. However, conventional motion analysis has not been widely used to this end because it requires special equipment and markers need to be placed on the whole body of the patient. If human activities in various environments could be analyzed with markerless video data, the benefits would be significant. Therefore, we compared OpenPose (a markerless method) with conventional PMMC by using the lower limb joint angles as indices. Under the

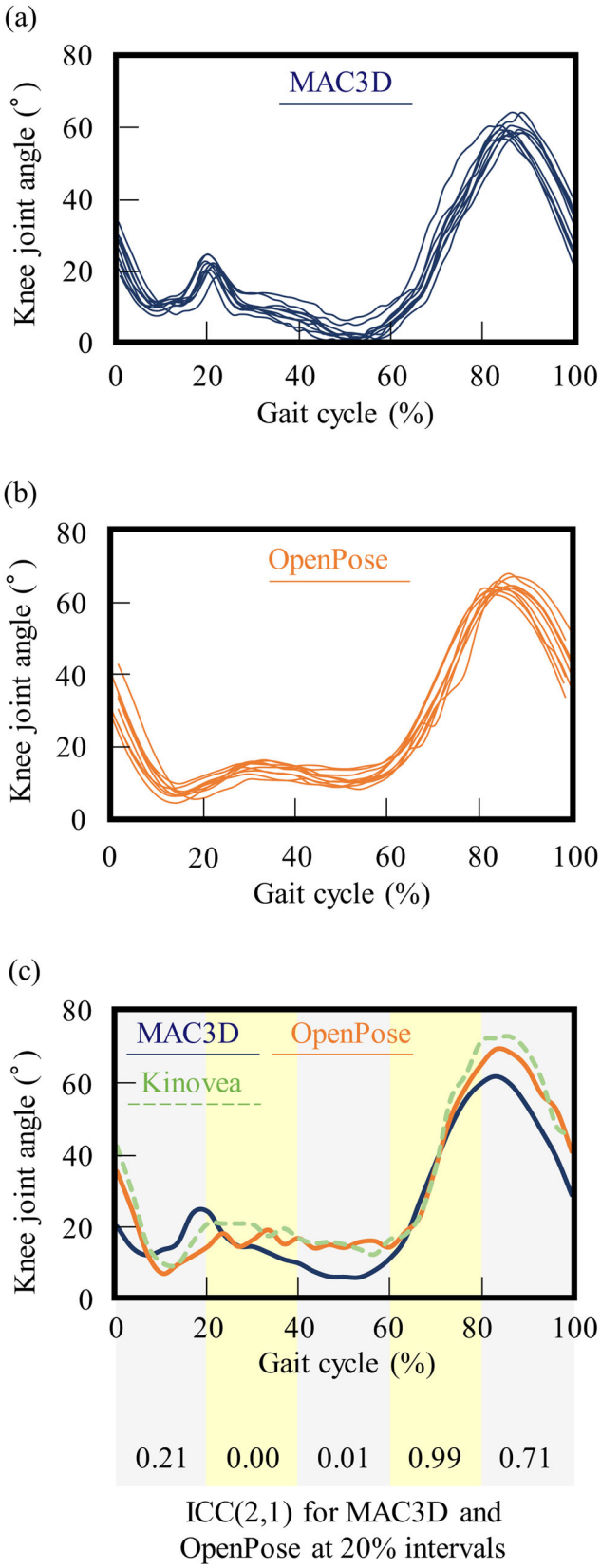

Figure 4. Left knee joint angle results. (a), (b) Ten superimposed gait cycles determined by MAC3D and OpenPose, respectively. (c) Superimposed left knee joint angles of a typical gait obtained by MAC3D, OpenPose, and Kinovea.

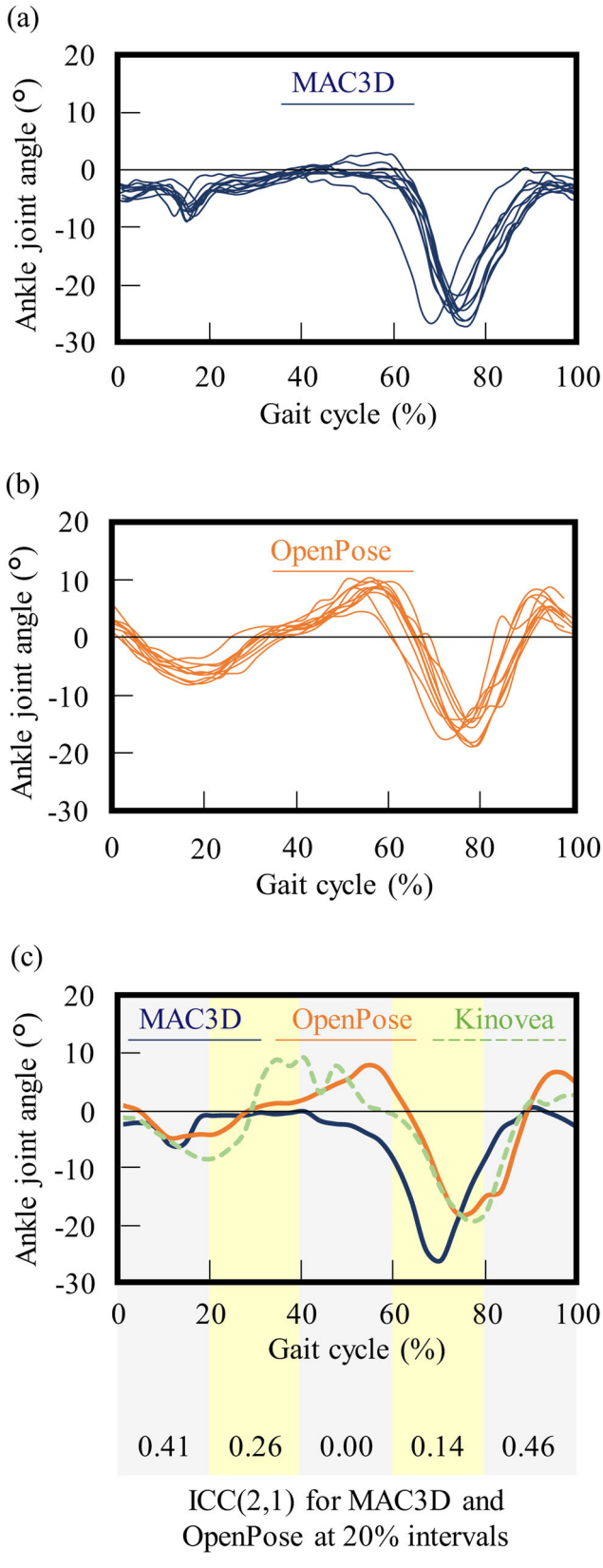

Figure 5. Left ankle joint angle results. (a), (b) Ten superimposed gait cycles determined by MAC3D and OpenPose, respectively. (c) Superimposed left ankle joint angles of a typical gait obtained by MAC3D, OpenPose, and Kinovea.

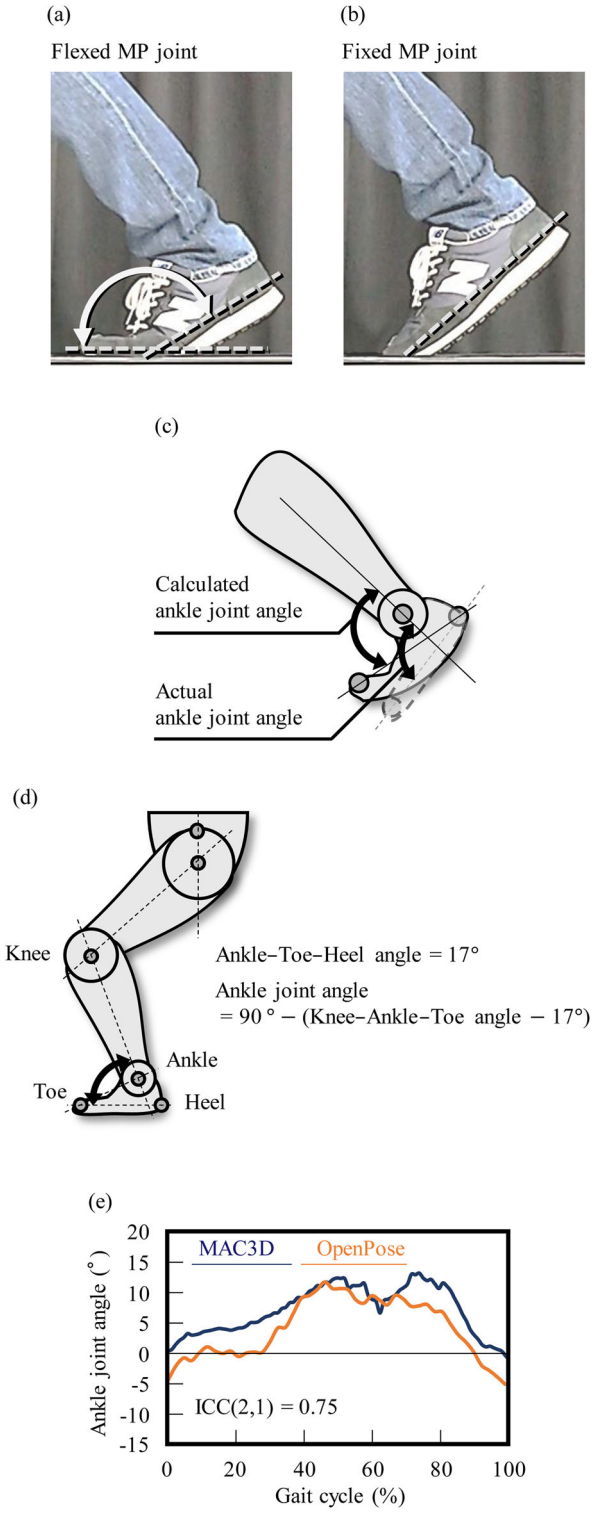

Figure 6. Effect of metatarsophalangeal (MP) joint restraint on the analysis results of the ankle joint angle. Treadmill gait with (a) normal (unrestrained) MP joint motion and (b) restrained MP joint motion by the use of metal insoles. (c) Schematic of MP joint flexion during walking; as the MP joint flexes in the terminal stance phase of normal gait, the definition of the ankle joint angle shown in Figure 2 cannot be applied. (d) New definition of the ankle joint angle; when the MP joint is fixed, the Ankle–Toe–Heel angle is constant (17°). (e) Left ankle joint angle changes in a gait cycle when metal insoles are used to minimize the influence of the MP joint angle change.

condition of recording the subject's motion on the focal plane of a single video camera, the hip and knee joint angles during walking were strongly correlated for both methods. In the case of the ankle joint angle, however, its intraclass correlation coefficient ICC (2,1) was lower than that of the hip and knee joints. As shown in Figure 2, the coordinates of the knee joint, ankle joint, toe, and heel were used to calculate the ankle joint angle. Since this angle was strongly correlated for MAC3D, the positions of the knee joint and ankle joint were almost the same for OpenPose and MAC3D because they were used for the calculation of the knee joint angle. Therefore, the discrepancy in the ankle joint angle was caused by the detection position of the heel and/or toe. Conventional PMMC methods, such as MAC3D, estimate the positions of the actual body parts from the positions of the markers on the body surface. On the other hand, AI-assisted methods and Kinovea estimate those positions directly from video data. Therefore, it is assumed that the differences in the positions of the heel and toe were caused by such methodological differences.

Previous studies have also attempted to analyze human motion without using markers; Microsoft Kinect has been used to detect human body parts using an infrared depth sensor. Eltoukhy et al. (2017) compared the conventional PMMC system with the Kinect method for joint angle and step length determination during treadmill walking. In their study, the maximum ICC (2,1) for the range of motion of the hip, knee, and ankle joints were 0.80, 0.80, and 0.05, respectively. Oh et al. (2018) studied stair ascent and descent motions; the maximum ICC (2,1) values for the aforementioned joints were 0.86, 0.90, and 0.49, respectively. These studies also reported lower correlations between the markerless method and the conventional PMMC system; however, the analysis results of OpenPose were significantly more accurate. The inaccurate ankle joint results of Kinect could be owing to the difference in the definition of the ankle joint angle (Eltoukhy et al. 2017; Oh et al. 2018). As the ankle and toe are the only key points of the foot that Kinect can recognize, many studies defined the angle between the knee, ankle, and toe as the ankle joint angle. However, the ankle angle should be defined as the angle between the line connecting the knee joint and ankle joint and the line connecting the toe and heel, as shown in Figure 2 (Grill and Mortimer 1996; Surer et al. 2011; Romain and Xuguang 2012; Chen et al. 2013).

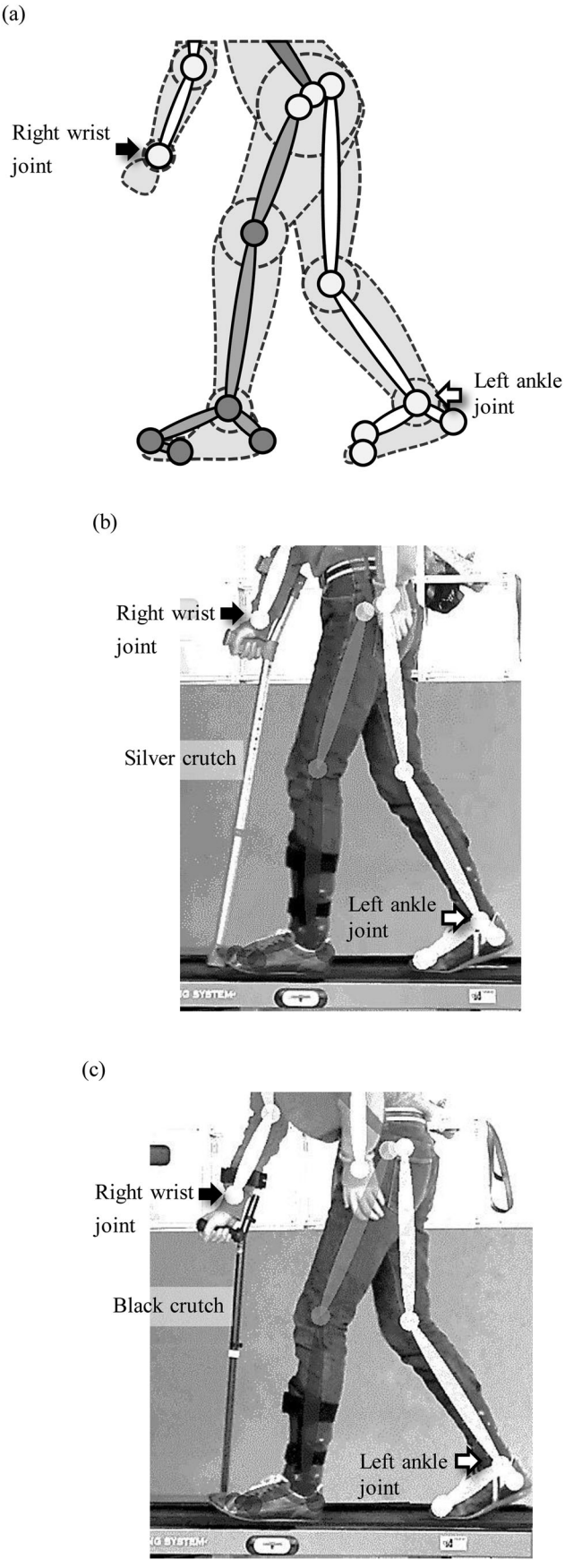

Figure 7. Recognition results of OpenPose during treadmill walking. (a) Analysis results represented by connected circles and lines. (b) Silver and (c) black Lofstrand crutch results.

As shown in Figure 4(c), double knee action was not seen in the case of OpenPose. The double knee action is a typical angular change in the knee joint during walking. It consists of the first peak in the stance phase and the second peak in the swing phase. The former is for absorbing the impact when the leg touches the ground. It is possible that the tilt of the leg in relation to the walking direction may cause the flexion angle to be estimated as smaller than it should be. The maximum tilt angles from the walking direction of the thigh, shank, and foot at the first peak of double knee action (approximately 15 to 25% of the gait cycle) were 25, 24, and 42 degrees, respectively. In contrast, those at the second peak (approximately 65 to 100% of the gait cycle) were 38, 14, and 7 degrees, respectively. In the interval of the second peak, the general shapes of the graphs of MAC3D and OpenPose are similar and the ICC (2,1) value is closer to one. Thus, accurate analysis by OpenPose requires that the subject's motion be restricted to the plane as much as possible.

As shown in Figure 6, the MP joint flexes during the terminal stance phase (approximately 40–60% of the gait cycle) in normal gait. In this case, the definition of the ankle joint angle shown in Figure 2 cannot be applied, and the calculated ankle joint angle deviates from the actual value (Figure 6(c)). When the MP joint was fixed, the definition of ankle joint angle shown in Figure 2 was satisfied throughout the gait cycle and the ankle joint angles during gait correlated well between OpenPose and MAC3D. These results indicate that AI-assisted markerless motion capture is more suitable under the fixed MP joint condition than under the normal condition. Furthermore, as the ankle foot orthosis and crutch did not affect the recognition accuracy of OpenPose, this method is suitable for motion capture analysis of patients suffering from gait disturbance.

It should be noted that the hip, knee, and ankle joint angles calculated from the data obtained by OpenPose and Kinovea were highly similar: the ICC (2,1) values for the hip, knee, and ankle joint angles for OpenPose and Kinovea were 0.98, 0.98, and 0.87, respectively. This indicates that the body part recognition ability of OpenPose is significantly high.

The results of this study prove that motion analysis using a single camera is an adequate alternative to the conventional PMMC system when the subject's motion is limited to a two-dimensional plane. If it is necessary to recognize the movements of both legs, such as in the analysis of gait disturbance, a second camera can be placed in an opposing position. By

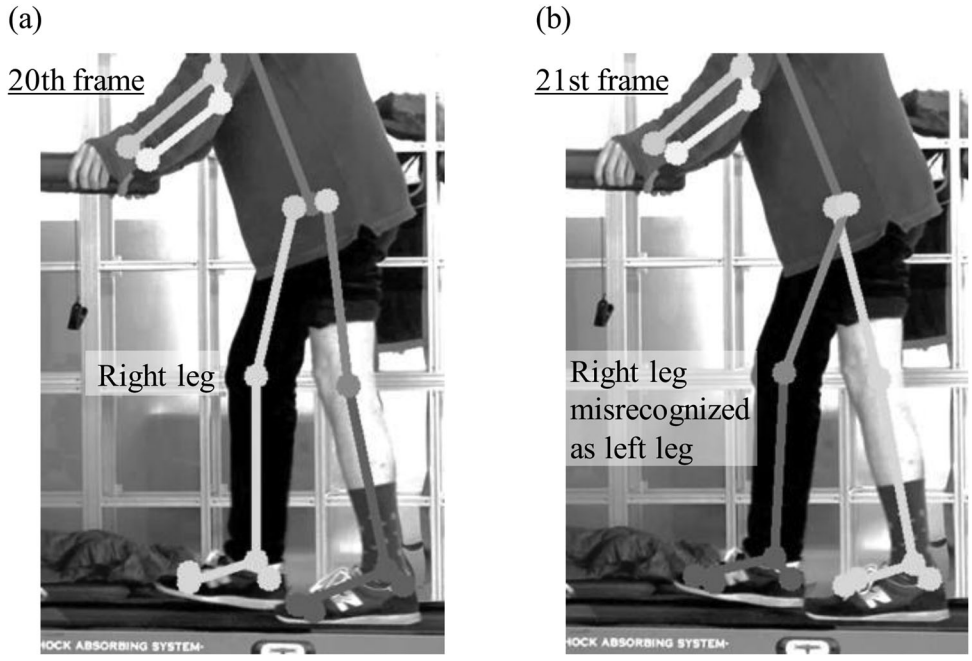

Figure 8. OpenPose's recognition error. (a) OpenPose correctly recognizes the right and left legs. (b) The right and left legs are reversely recognized.

using multi-cameras, AI-assisted motion capture software could achieve a higher resolution and three-dimensional coordinate analysis accuracy (Rhodin et al. 2018). The advantage of markerless motion capture lies in the freedom of the recording environment, which also enables the analysis of the subject's natural motion without the restrictions caused by body markers. As OpenPose analyzes each video frame, videos such as those of sports and falling accidents could be analyzed. Taking into consideration characteristic limitations such as right/left reverse recognition, AI-assisted markerless motion capture software is an attractive substitute for conventional motion capture systems.

5. Conclusion

OpenPose can be an adequate alternative to conventional PMMC when the motion of the subject is limited to a two-dimensional plane. AI-assisted markerless motion capture is also suitable for analyzing gait disturbance, such as the fixed MP joint condition. The use of an ankle foot orthosis and a crutch did not influence the body part recognition accuracy of OpenPose. Therefore, OpenPose is useful for the motor analysis of patients suffering from gait disturbance. In addition, by using OpenPose, the aforementioned limitations of the conventional PMMC method could be overcome without compromising recognition accuracy.

Declaration of interest statement

There is no declaration of interest statement.

Funding

This study was supported by Center Of Innovation (COI) programs of Japan Science and Technology Agency, Japan Society for the Promotion of Science Grant-in-Aid for Early-Career Scientists (JP19K19865), and grant-in-aid for work-related injuries of Ministry of Health, Labor and Welfare (190401).

ORCID

Iwori Takeda http://orcid.org/0000-0003-4973-0429

References

Alkjaer T, Simonsen EB, Dyhre-Poulsen P. 2001. Comparison of inverse dynamics calculated by two- and three-dimensional models during walking. Gait Posture. 13(2):73–77.

Cao Z, Simon T, Wei SE, Sheikh Y. 2017. Realtime multi-person 2D pose estimation using part affinity fields. Proc - 30th IEEE Conf Comput Vis Pattern Recognition, CVPR 2017. 2017-Janua(Xxx):1302–1310.

Chen M, Wu B, Lou X, Zhao T, Li J, Xu Z, Hu X, Zheng X. 2013. A self-adaptive foot-drop corrector using functional electrical stimulation (FES) modulated by tibialis anterior electromyography (EMG) dataset. Med Eng Phys. 35(2):195–204. http://dx.doi.org/10.1016/j.medengphy.2012.04.016.

Cicchetti DV. 1994. Guidelines, criteria, and rules of thumb for evaluating normed and standardized assessment instruments in psychology. Psychol Assess. 6(4):284–290. [accessed 2019 Oct 28] http://doi.apa.org/getdoi.cfm?doi=10.1037/1040-3590.6.4.284.

Dahlgren G, Carlsson D, Moorhead A, Häger-Ross C, McDonough SM. 2010. Test-retest reliability of step counts with the ActivPAL™ device in common daily activities. Gait Posture. 32(3):386–390.

Eltoukhy M, Oh J, Kuenze C, Signorile J. 2017. Improved kinect-based spatiotemporal and kinematic treadmill gait assessment. Gait Posture. 51:77–83. http://dx.doi.org/10.1016/j.gaitpost.2016.10.001.

Fang HS, Xie S, Tai YW, Lu C. 2017. RMPE: Regional Multi-person Pose Estimation. Proc IEEE Int Conf Comput Vis. :2353–2362.

Grill WM, Mortimer JT. 1996. Quantification of recruitment properties of multiple contact cuff electrodes. IEEE Trans Rehabil Eng. 4(2):49–62.

Kendall A, Grimes M, Cipolla R. 2015. PoseNet: A convolutional network for real-time 6-dof camera relocalization. Proc IEEE Int Conf Comput Vis. :2938–2946.

Lee HJ, Lee S, Chang WH, Seo K, Shim Y, Choi BO, Ryu GH, Kim YH. 2017. A Wearable Hip Assist Robot Can Improve Gait Function and Cardiopulmonary Metabolic Efficiency in Elderly Adults. IEEE Trans Neural Syst Rehabil Eng. 25(9):1549–1557.

Lichtwark GA, Bougoulias K, Wilson AM. 2007. Muscle fascicle and series elastic element length changes along the length of the human gastrocnemius during walking and running. J Biomech. 40(1):157–164.

Matić A, Petrović Savić S, Ristić B, Stevanović VB, Devedžić G. 2016. Infrared assessment of knee instability in ACL deficient patients. Int Orthop. 40(2):385–391.

McMulkin ML, Mader S, Elizondo T, Baird GO. 2019. Quantitative coronal plane motion of hindfoot during clinical flexibility assessments. Gait Posture. 71(February):116–119..

Mehrizi R, Peng X, Metaxas DN, Xu X, Zhang S, Li K. 2019. Predicting 3-D lower back joint load in lifting: A deep pose estimation approach. IEEE Trans Human-Mach Syst. 49(1):85–94.

Nakano N, Sakura T, Ueda K, Omura L, Kimura A, Iino Y, Fukashiro S, Yoshioka S. 2019. Evaluation of 3D markerless motion capture accuracy using OpenPose with multiple video cameras. bioRxiv: 842492. http://biorxiv.org/content/early/2019/11/15/842492.abstract.

Namba HF, Brinkman WM, Meijer RP, Koldewijn EL, Basten V, Bangma C, Wagner C. 2020. Analysis of the video motion tracking system 'Kinovea' to assess surgical movements during robot-assisted radical prostatectomy.

Oh J, Kuenze C, Jacopetti M, Signorile JF, Eltoukhy M. 2018. Validity of the Microsoft Kinect™ in assessing spatiotemporal and lower extremity kinematics during stair ascent and descent in healthy young individuals. Med Eng Phys. 60:70–76..

Patterson MR, Whelan D, Reginatto B, Caprani N, Walsh L, Smeaton AF, Inomata A, Caulfield B. 2014. Does external walking environment affect gait patterns? 2014 36th Annu Int Conf IEEE Eng Med Biol Soc EMBC. 2014:2981–2984.

Post A, Koncan D, Kendall M, Cournoyer J, Michio Clark J, Kosziwka G, Chen W, de Grau Amezcua S, Blaine Hoshizaki T. 2018. Analysis of speed accuracy using video analysis software. Sports Eng. 21(3):235–241..

Qiao S, Wang Y, Li J. 2017. Real-time human gesture grading based on OpenPose. In: 2017 10th Int Congr Image Signal Process Biomed Eng Informatics [Internet]. [place unknown]: IEEE; [accessed 2019 Oct 28]; p. 1–6. http://ieeexplore.ieee.org/document/8301910/.

Rhodin H, Meyer F, Spörri J, Muller E, Constantin V, Fua P, Katircioglu I, Salzmann M. 2018. Learning Monocular 3D Human Pose Estimation from Multi-view Images. Proc IEEE Comput Soc Conf Comput Vis Pattern Recognit. :8437–8446.

Romain P, Xuguang W. 2012. Development of objective discomfort evaluation indicators for a task-oriented motion using less constrained motion concept: Application to automotive pedal clutching task. Work. 41(SUPPL.1):1461–1465.

Saini N, Price E, Tallamraju R, Enficiaud R, Ludwig R, Martinovic I, Ahmad A, Black M. 2019. Markerless Outdoor Human Motion Capture Using Multiple Autonomous Micro Aerial Vehicles. Proc IEEE/CVF Int Conf Comput Vis; p. 823–832.

Slembrouck M, Luong H, Gerlo J, Schütte K, Van Cauwelaert D, De Clercq D, Vanwanseele B, Veelaert P, Philips W. 2020. Multiview 3D Markerless Human Pose Estimation from OpenPose Skeletons. In: Blanc-Talon J, Delmas P, Philips W, Popescu D, Scheunders P, editors. Adv Concepts Intell Vis Syst. Cham: Springer International Publishing; p. 166–178.

Surer E, Cereatti A, Grosso E, Croce U. Della 2011. A markerless estimation of the ankle-foot complex 2D kinematics during stance. Gait Posture. 33(4):532–537. http://dx.doi.org/10.1016/j.gaitpost.2011.01.003.